



24 May 2002

**CHEMICAL  
PHYSICS  
LETTERS**

Chemical Physics Letters 358 (2002) 71–76

www.elsevier.com/locate/cplett

# Rate coefficients for photoinitiated NO<sub>2</sub> unimolecular decomposition: energy dependence in the threshold regime

D. Stolyarov, E. Polyakova, I. Bezel<sup>1</sup>, C. Wittig<sup>\*</sup>

*Department of Chemistry, University of Southern California, Los Angeles, CA 90089-1062, USA*

Received 10 December 2001; in final form 13 March 2002

## Abstract

Rate coefficients  $k(E)$  for photoinitiated NO<sub>2</sub> unimolecular decomposition have been obtained by recording the product NO laser-induced fluorescence signal intensity versus the delay between the pump and probe pulses. A 10 ps pump-probe cross-correlation temporal width provides a useful compromise between time and frequency resolution ( $3\text{ cm}^{-1}$ ).  $k(E)$  increases rapidly: from  $\sim 2 \times 10^{10}$  to  $\geq 1.3 \times 10^{11}\text{ s}^{-1}$  within  $25\text{ cm}^{-1}$  of reaction threshold. In this regime, long-range interfragment interactions play an important role. A high level of theory will be needed to reconcile these results. © 2002 Published by Elsevier Science B.V.

## 1. Introduction

The unimolecular decomposition of small polyatomic molecules via barrierless path ways continues to present intellectual challenges, with NO<sub>2</sub> being a benchmark system for such studies. The situation is particularly intriguing at energies ( $E$ ) that lie just above reaction threshold ( $D_0 = 25128.57 \pm 0.05\text{ cm}^{-1}$  [1,2]), where a modest number of independent reactive channels are energetically accessible. For example, at energies that

are barely in excess of a given channel threshold, the corresponding de Broglie wavelength for interfragment translational motion exceeds any of the linear dimensions of the molecule's equilibrium geometry. Consequently, the transition state (TS) region for this channel is comparably large, underscoring the need for a fully quantum mechanical treatment of the dynamics.

In consideration of the above, it is inevitable that properties of the reacting system are sensitive to the long-range interfragment potential. Moreover, the convergence of potential energy surfaces (PESs) correlating to the same products at large values of the interfragment separation ( $r$ ) needs to be taken into account, in contrast to the situation at higher energies and correspondingly smaller  $r$  values. For example, PESs that are repulsive at short range can be attractive at large  $r$  values [3],

<sup>\*</sup> Corresponding author. Fax: +1-213-746-4945.

*E-mail addresses:* [ilya@xenon.cchem.berkeley.edu](mailto:ilya@xenon.cchem.berkeley.edu) (I. Bezel), [wittig@usc.edu](mailto:wittig@usc.edu) (C. Wittig).

<sup>1</sup> Present address: Miller Institute for Basic Research in Science, 2536 Channing Way, Berkeley, CA 94720, USA.

thereby contributing to a marked increase in the molecular density of states ( $\rho$ ) in the threshold regime [4–6]. This singular behavior of  $\rho$  affects profoundly the reaction rate coefficients.

In a previous publication [7], experimental results were presented in which ‘nearly-microcanonical’ (i.e.,  $\sim 2 \text{ cm}^{-1}$  resolution) rate coefficients  $k(E)$  for the unimolecular decomposition of expansion-cooled, photoexcited  $\text{NO}_2$  molecules were measured at energies just above  $D_0$ . It was shown that  $k(E)$  increases rapidly, i.e., from  $\sim 2 \times 10^{10}$  to  $\geq 10^{11} \text{ s}^{-1}$  over a range of approximately  $17 \text{ cm}^{-1}$ . The smaller  $k(E)$  values are consistent with spectroscopic measurements that have been carried out just above  $D_0$ , where some, albeit minimal, spectral resolution is possible [4,8]. The larger  $k(E)$  values are consistent with ultrafast time-domain measurements, in which large laser linewidths (typically  $\sim 30 \text{ cm}^{-1}$  FWHM) precluded the possibility of examining energies that lie just above  $D_0$  [9–11].

The  $\text{NO}_2$  system has provided the only experimental verification to date of the rapid increase of  $k(E)$  above its reaction threshold that is anticipated for barrierless reactions on the basis of long-range interactions. In our earlier paper [7], time and energy resolution were limited by the 25 ps pump-probe cross-correlation temporal width (hereafter referred to as the temporal width) and the pump laser linewidth of  $\sim 2 \text{ cm}^{-1}$ . This enabled the smallest  $k(E)$  values (i.e.,  $\sim 2 \times 10^{10} \text{ s}^{-1}$ ) to be measured with acceptable accuracy. However, because of the 25 ps temporal width, these measurements provided only rough estimates for  $k(E)$  values that are comparable to the inverse of the temporal width. Consequently, a lower bound was recommended for  $k(E)$  values  $\geq 10^{11} \text{ s}^{-1}$ .

The manner in which the molecular density of states enters transition state theory (TST) models (e.g., RRKM theory) requires that regions are identified as the molecular, TS, and product spaces [12]. The location of the TS region along the reaction coordinate depends on  $E$ , and this dependence can be strong for barrierless reactions. In this case, the reaction rate coefficient per open channel excluding tunneling ( $1/h\rho$ ) can be said to increase with  $E$  from a TST perspective. Namely, as the TS region moves to smaller  $r$ , the portion of the phase space volume that is due to the long-

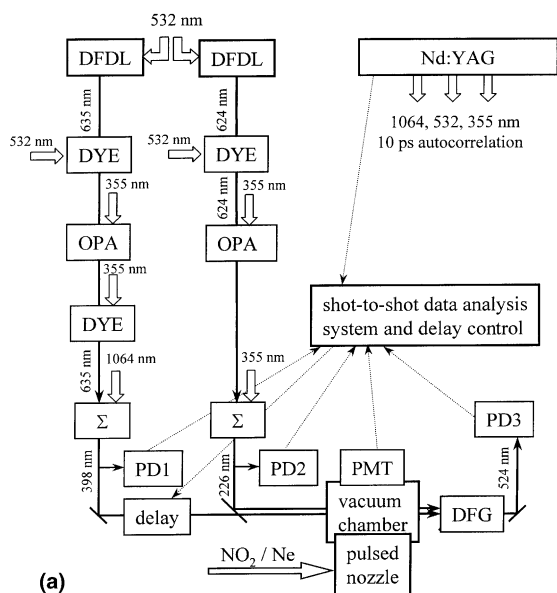
range part of the potential is eliminated from the molecular space, thus causing  $\rho$  to decrease [7].

In this Letter,  $k(E)$  values are presented for the threshold region:  $0 \leq E - D_0 \leq 27 \text{ cm}^{-1}$ . Relative to our earlier measurements [7], expansion cooling has been improved markedly (i.e.,  $\sim 1 \text{ K}$  versus  $\sim 5 \text{ K}$ ), thus eliminating uncertainties that arise because of the occupation of low-lying parent rotational levels. In addition, the temporal width has been shortened from 25 to 10 ps, thereby improving the accuracy with which the larger rates can be determined, albeit with a slight loss of spectral resolution (i.e.,  $\sim 2 \text{ cm}^{-1}$  versus  $3 \text{ cm}^{-1}$ , respectively). This has also enabled a larger energy range to be examined. A dramatic increase of  $k(E)$  is observed near  $25152 \text{ cm}^{-1}$ , which is  $23 \text{ cm}^{-1}$  above  $D_0$ . These results provide a challenge to theoretical models, which to date have been able to rationalize results obtained at higher  $E$  (and therefore smaller  $r$  values) by using conventional statistical theories [12], but have yet to model quantitatively the threshold regime.

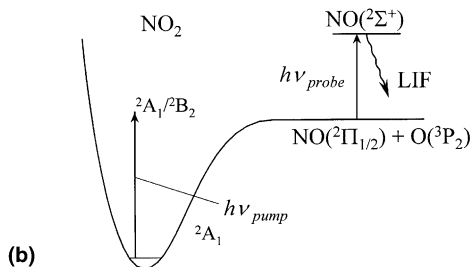
## 2. Experimental

Much of the experimental arrangement has been reported previously [7,11]. Referring to Fig. 1a, the  $\sim 400 \text{ nm}$  pump and  $226 \text{ nm}$  probe pulses are obtained by up-converting the outputs of two distributed feedback dye lasers (DFDLs). A  $\sim 30 \text{ ps}$  Nd:YAG laser (EXPLA PL2143C) served as the pump source for the DFDLs and amplifiers and provided  $1064$  and  $355 \text{ nm}$  pulses for frequency mixing. The cross-correlation of the pump and probe pulses was measured simultaneously with the signal by generating a difference frequency (near  $524 \text{ nm}$ ) in a BBO crystal. These cross-correlation scans were used in the fitting routine, which has been described elsewhere [11].

The changes to the laser system are summarized here. First, the optical scheme of the Nd:YAG laser was altered in order to shorten its pulses. As a result, the pump-probe cross-correlation temporal width decreased from 25 to 10 ps. Because of a concomitant loss of energy, side-pumped dye cells were introduced into the pump and probe branches. The  $5 \text{ mm}$  BBO crystal used for the



(a)



(b)

Fig. 1. (a) Schematic diagram of the experimental arrangement. Acronyms are defined as follows: DFDL – distributed feedback dye laser; DYE – dye amplifier; OPA – optical parametric amplifier;  $\Sigma$  – sum frequency generation; PD – photodiode; DFG – difference frequency generation; PMT – photomultiplier tube. (b) Photoinitiated  $\text{NO}_2$  unimolecular decomposition is monitored by detecting the NO product via  $\text{A}^2\Sigma^+ \leftarrow \text{X}^2\Pi_{1/2}$  LIF as the pump-probe delay is varied. The excited  $^2\text{B}_2$  and ground  $^2\text{A}_1$  electronic states of  $\text{NO}_2$  are strongly mixed, resulting in vibronic manifolds having  $\text{A}_1$  and  $\text{B}_2$  symmetries, which only interact via rotation.

cross-correlation measurements was replaced with a 0.5 mm one in order to improve the temporal resolution of the cross-correlator. Frequency drift of the DFDLs [7] was minimized by careful adjustment of an active temperature stabilization system. Frequency measurements of the pump pulse were carried out by using a wavemeter (Burleigh WA-4500) calibrated by using its internal He–Ne laser. The DFDL output (after ampli-

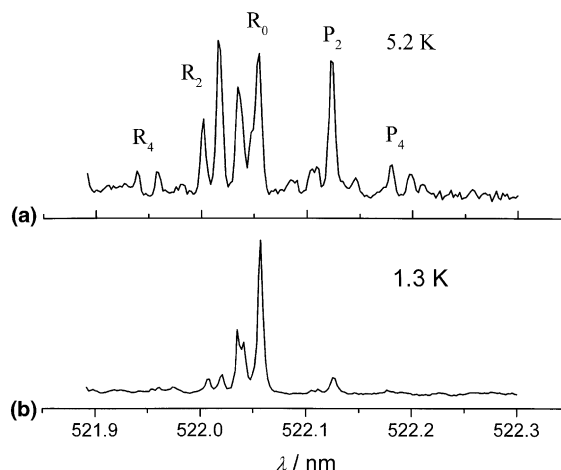


Fig. 2. Rotational temperatures are determined by using LIF of the  $\text{NO}_2$  absorption feature near 522 nm. The upper trace was recorded under conditions similar to those used previously [7]. The lower trace is representative of the conditions used in the work reported herein.

fication in the dye cell) was measured because the wavemeter is more accurate at longer wavelengths. The pump pulse spectral width was found to be approximately  $3 \text{ cm}^{-1}$ .

The pump-probe scenario is presented in Fig. 1b. In our previous measurements, expansion-cooled samples (0.6%  $\text{NO}_2$  in He at 3 bar) had rotational temperatures ( $T_{\text{rot}}$ ) of  $\sim 5 \text{ K}$  [7]. Thus, several low-lying rotational levels were occupied. Rotational temperatures of  $\sim 1 \text{ K}$  have been achieved in the work reported here by using 0.02%  $\text{NO}_2$  in Ne at 7 bar. Laser-induced fluorescence (LIF) near 522 nm was used to obtain rotational temperatures (Fig. 2); a spectrum was recorded prior to starting rate coefficient measurements at each new pump wavelength, and the expansion conditions were held constant throughout the ensuing experiment.  $\text{NO}_2$  samples (Matheson, 99.5%) were purified prior to each set of experiments by bubbling  $\text{O}_2$  through cooled liquid  $\text{NO}_2$  samples.

### 3. Results

Fig. 3 shows typical data (open circles) of LIF signal intensity versus pump-probe delay,  $\tau_{\text{delay}}$ , for

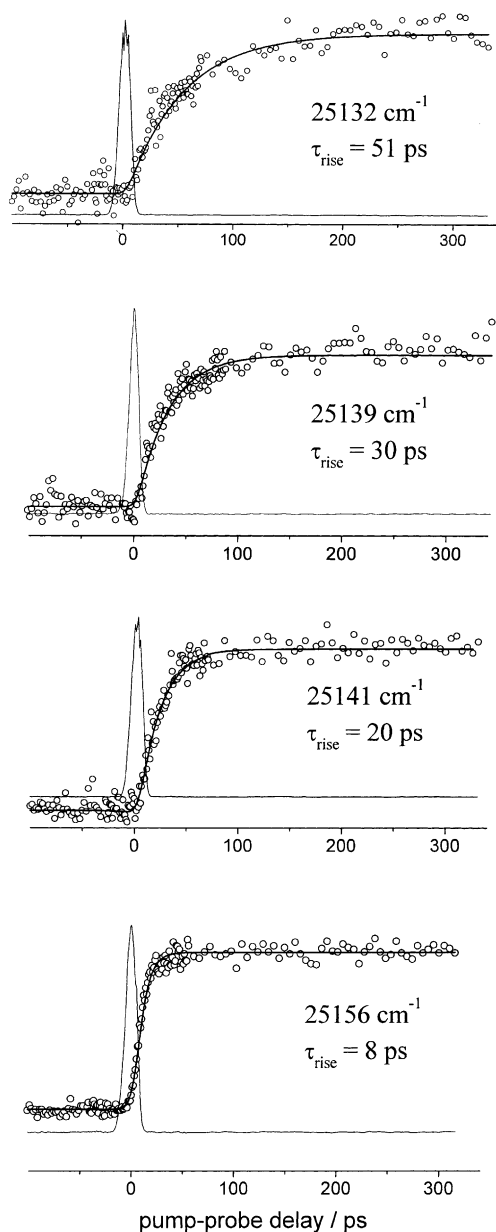


Fig. 3. Typical data showing LIF signal intensity (open circles) versus pump-probe delay. The  $\tau_{\text{rise}}$  values were obtained by fitting the data to a single exponential rise [11]. The corresponding cross-correlations are shown as thin solid lines. Note the pronounced variation of the  $\tau_{\text{rise}}$  values with  $E$ .

four different values of the ‘center energies’ of the pump-laser photons. The pump-probe cross-correlations are shown as the thin solid traces. The

molecular response, whose convolution with the cross-correlation yields the observed signal, is assumed to be proportional to  $1 - \exp\{-t/\tau_{\text{rise}}\}$ . The  $\tau_{\text{rise}}$  values are obtained by using the fitting procedure that has been described previously [11], which yields the solid-line fits to the data shown in Fig. 3. The  $k(E)$  values are taken to be the  $\tau_{\text{rise}}^{-1}$  values. The rapid increase of  $k(E)$  with  $E$  throughout this modest energy range is striking.

Fig. 4 shows  $k(E)$  for  $E$  values that range from the reaction threshold to 25155  $\text{cm}^{-1}$ . A steady increase is observed, albeit with point-to-point fluctuations that increase with  $E$ . The smallest  $\tau_{\text{rise}}$  values extracted from the fits are smaller than the  $\sim 10$  ps cross-correlation widths, and therefore are

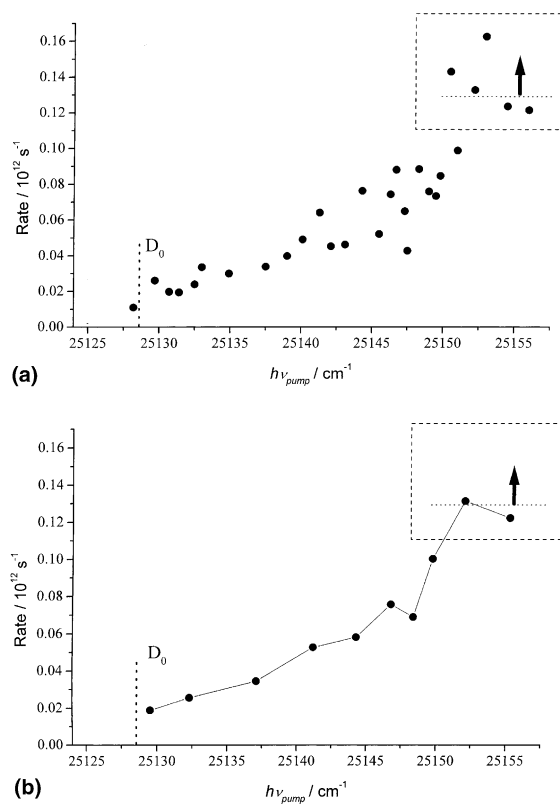


Fig. 4. (a) Rate coefficient versus  $E$  for the threshold regime. (b) The result of three-point smoothing of the data in (a). Vertical dashed lines indicate  $D_0$ . At the largest  $E$  values, the  $\tau_{\text{rise}}$  values are too small to be reliable. A lower bound of  $1.3 \times 10^{11}$  is assigned to the corresponding rates; see text for details.

of insufficient accuracy. Thus, referring to Fig. 4, the rate measurements at the largest  $E$  values are assumed to yield a lower bound of  $1.3 \times 10^{11}$ , which is obtained by averaging the  $\tau_{\text{rise}}$  values and then taking the inverse. This is indicated by the boxed region and the thick arrow, which denotes  $k \geq 1.3 \times 10^{11}$ . Likewise, large point-to-point fluctuations between 25 145 and 25 150  $\text{cm}^{-1}$  are attributed mainly to the inability to uniquely deconvolute the data. In addition, if the density of molecular states decreases, as discussed below, fluctuations may also occur because a modest number of resonances are excited by the 3  $\text{cm}^{-1}$  pump pulse. For example, if the extrapolated vibronic density of states of 0.4  $\text{cm}^{-1}$  is used [5,13], the 3  $\text{cm}^{-1}$  pump beam excites only a few resonances, in which case fluctuations are inevitable.

The quality of the experimental data does not support a multi-exponential fit. In Fig. 4b, the data have been subjected to a three-point smoothing routine. The results shown in Fig. 4 are in agreement with those reported previously [7], with account taken of the different rotational temperatures.

#### 4. Discussion

The data presented in Fig. 4 show that for expansion-cooled, photoexcited  $\text{NO}_2$ ,  $k(E)$  increases by an order of magnitude over a modest energy interval of  $\sim 20 \text{ cm}^{-1}$  above  $D_0$ . The small  $k$  values obtained when  $E$  is slightly in excess of  $D_0$  (i.e.,  $\sim 2 \times 10^{10} \text{ s}^{-1}$ ) can be rationalized on the basis of long-range interactions that play a role in the threshold regime, as discussed previously [7]. These interactions account for the rate coefficients being an order of magnitude smaller than those calculated on the basis of an extrapolation of the density of states [13,14].

The laser linewidth of 3  $\text{cm}^{-1}$  used in the work reported here averages over a number of resonances, thereby lessening the fluctuations of the observed rates that arise as a consequence of the quantum-chaotic nature of the intramolecular dynamics. Earlier studies that have used ultrafast pulses whose linewidths are  $\sim 30 \text{ cm}^{-1}$  have yielded energy-averaged rate coefficients of approximately  $1.6 \times 10^{11} \text{ s}^{-1}$  in the threshold region [9],

which is an order of magnitude larger than the smallest rates reported here. A reconciliation of the small  $k(E)$  values reported here for energies of several  $\text{cm}^{-1}$  above  $D_0$  and the  $1.6 \times 10^{11} \text{ s}^{-1}$  value reported earlier, requires that a dramatic increase of  $k(E)$  occurs with increasing  $E$ . Indeed, this is observed.

In the statistical theory of unimolecular decomposition, the rate for each independent open channel is given by  $1/h\rho$  when tunneling is unimportant, as is the case for barrierless reactions, where  $\rho$  is the density of strongly coupled *molecular* states that participate in the reaction [12]. When using this expression, it has generally been assumed that  $\rho$  remains approximately constant over modest energy intervals, such as the tens of  $\text{cm}^{-1}$  encountered in the work reported herein. For barrierless reactions, however, the molecular and product regions are separated by a TS region whose location along the reaction coordinate varies strongly with  $E$  in the threshold region of each open channel. Thus,  $\rho$  can be a function of the location of the TS, and consequently  $\rho$  can have a significant energy dependence near threshold.

In this regime, the use of conventional TST to describe variations of the rate must be questioned. Indeed, even the definition of the average rate in such systems is subjective, because it depends on the energy interval over which the rates are averaged. In the context of  $\text{NO}_2$  decomposition [7], it has been argued that the couplings that occur at large interfragment separation should be ‘counted’ in the molecular space for  $E$  values that are barely in excess of  $D_0$  but in the product space for higher  $E$  values. Thus, the corresponding density of molecular states can change with  $E$ , even if the number of open channels does not. Such complexity of the coupling hierarchy and the rapid energy variation of the definition of the molecular phase space lies beyond the use of statistical theories or classical approaches to calculate reaction rates. Though qualitative insight can be gained, there is limited value in manipulating these models in order to fit data. Quantum mechanical calculations that include the participation of multiple PESs are likely to yield results that provide the best insights into how these threshold reactions occur.

## 5. Summary

The data reported herein are grist for the mill of theory. The current measurements provide a good compromise between time and energy resolution for the threshold regime. The physical basis for the observed threshold behavior, in which  $k(E)$  is an order of magnitude smaller for  $E$  values in slight excess of  $D_0$  than predictions based on  $\rho$  values obtained hundreds of  $\text{cm}^{-1}$  below  $D_0$ , has been identified at a qualitative level. This phenomenon is expected to be general, applying to a number of molecules that undergo unimolecular decomposition via loose TSs. It may also be relevant to evaporation at ultralow temperatures, for example from  $^3\text{He}$  and  $^4\text{He}$  clusters.

## Acknowledgements

This research has been supported by the National Science Foundation (CHE 9800761). We have had valuable discussions with H. Reisler.

## References

- [1] R. Jost, J. Nygård, A. Pasinski, A. Delon, J. Chem. Phys. 105 (1996) 1287.
- [2] R. Jost, J. Nygård, A. Pasinski, A. Delon, Phys. Rev. Lett. 78 (1997) 3093.
- [3] H. Katagiri, S. Kato, J. Chem. Phys. 99 (1993) 8805.
- [4] J. Miyawaki, K. Yamanouchi, S. Tsuchiya, J. Chem. Phys. 99 (1993) 254.
- [5] A. Delon, S. Heilliette, R. Jost, Chem. Phys. 238 (1998) 465.
- [6] S.I. Ionov, H.F. Davis, E. Mikhaylichenko, L. Valachovic, R.A. Beaudet, C. Wittig, J. Chem. Phys. 101 (1994) 4809.
- [7] I. Bezel, D. Stolyarov, C. Wittig, J. Phys. Chem. A 103 (1999) 10268.
- [8] B. Abel, H.H. Hamann, N. Lange, Faraday Discuss. 102 (1995) 147.
- [9] S.I. Ionov, G.A. Brucker, C. Jaques, Y. Chen, C. Wittig, J. Chem. Phys. 99 (1993) 3420.
- [10] P.I. Ionov, I. Bezel, S.I. Ionov, C. Wittig, Chem. Phys. Lett. 272 (1997) 257.
- [11] I. Bezel, P. Ionov, C. Wittig, J. Chem. Phys. 111 (1999) 9267.
- [12] T. Baer, W.L. Hase, Unimolecular Reaction Dynamics: Theory and Experiments, Oxford University Press, New York, 1996.
- [13] R. Georges, A. Delon, R. Jost, J. Chem. Phys. 103 (1995) 1732.
- [14] A. Delon, R. Jost, M. Lombardi, J. Chem. Phys. 95 (1991) 5701.